ELSEVIER

Journal of Alloys and Compounds 323–324 (2001) 486–489

Journal of ALLOYS AND COMPOUNDS

www.elsevier.com/locate/jallcom

Study of the incommensurate–commensurate magnetic transition in $HoMnO_3$ perovskite

A. Muñoz[a,*], J.A. Alonso[b], M.T. Casais[b], M.J. Martínez-Lope[b], J.L. Martínez[b], M.T. Fernández[c]

[a]*Departamento de Física Aplicada, Escuela Politecnica Superior, Universidad Carlos III, Avda. Universidad, 30, Leganés, E-28911 Madrid, Spain*
[b]*Instituto de Ciencia de Materiales de Madrid, CSIC, Cantoblanco, E-28049 Madrid, Spain*
[c]*Institut Laue Langevin, BP 156X, Grenoble, 38042, France*

Abstract

The low-temperature magnetic structures of the orthorhombic perovskite $HoMnO_3$ have been studied on a polycrystalline sample from neutron diffraction, specific heat and susceptibility data. With cooling, $HoMnO_3$ exhibits three singularities at T_N=41 K, T≈26 K and T≈6.5 K, which suggests a rich magnetic phase diagram. At T_N, the Mn^{3+} magnetic moments become ordered in an incommensurate antiferromagnetic (AFM) arrangement, defined by a (C_x,0,0) mode, adopting a modulated sinusoidal magnetic structure which becomes commensurate with the unit cell below 29 K. Finally, below 22 K, an ordered magnetic moment appears on Ho^{3+} cations in an antiferromagnetic arrangement defined by a (A_x,0,C_z) mode; this moment significantly increases below 6.5 K, reaching a value of 7.27(11) μ_B at 1.8 K. The different magnetic structures are interpreted on the basis of competing superexchange interactions of opposite signs.

Keywords: Magnetically ordered materials; Neutron diffraction

1. Introduction

The mixed valence manganites showing colossal magnetoresistance [1,2] are based on the parent $RMnO_3$ perovskites (R=rare earths). They adopt the $GdFeO_3$ crystal structure, space group (*Pnma*), with $a \approx \sqrt{2}a_0$, $b \approx 2a_0$, $c \approx \sqrt{2}a_o$; a_0≈3.8 Å. Some research has been devoted to characterize the magnetic ground state of these undoped manganites. The best known member is the orthorhombic $LaMnO_3$ perovskite [3,4]: according to Hund's rules, the electronic configuration of the Mn^{3+} ions is $t_{2g}^3 e_g^1$. The e_g orbitals are strongly bonded with the oxygen p orbitals; a strong distortion of the MnO_6 octahedra associated with the Jahn–Teller effect breaks down the degeneracy of the e_g orbitals. This distortion seems to be in the origin of the orbital ordering observed in $LaMnO_3$. In the basal a–c plane, the dominantly populated $3dx^2$-$y^2/3dz^2$ orbitals alternate giving rise to a ferromagnetic (FM) superexchange interaction among the e_g orbitals within this a–c plane. The interlayer superexchange interaction is dominated by the interaction through the t_{2g} orbitals, which is AFM. At low temperatures these interactions stabilize a layered A-type AFM structure below T_N=140 K.

The $RMnO_3$ members for heavier rare earths have been, by far, much less studied. It is interesting to point out that, for rare earth cations smaller than Tb^{3+}, the orthorhombic perovskite structure for $RMnO_3$ is no longer the stable phase under ordinary synthetic conditions since a hexagonal non-perovskite phase (space group $P6_3cm$) with the same stoichiometry strongly competes in stability from Ho to Lu, Y and Sc. However, $HoMnO_3$ and $YMnO_3$ can be prepared as metastable phases by working under soft-chemistry conditions [5–7]. The aim of this work is to describe the magnetic ordering of the orthorhombic $HoMnO_3$.

2. Experimental

The $HoMnO_3$ perovskite was synthesized by thermal decomposition of citrate solutions of the involved cations, and a subsequent treatment in an O_2 flow at 900°C. Magnetic susceptibility was measured in a SQUID magnetometer. Neutron powder diffraction (NPD) diagrams were collected at the Institut Laue-Langevin (ILL) in Grenoble (France). To refine the crystallographic structure

*Corresponding author. Tel.: +34-91-624-9414; fax: +34-91-624-9430.

E-mail address: amunoz@elrond.uc3m.es (A. Muñoz).

0925-8388/01/$ – see front matter
PII: S0925-8388(01)01045-3

a high-resolution NPD pattern was acquired at room temperature at the D2B high-resolution diffractometer with λ=1.594 Å. A set of NPD patterns was obtained at D20 high-flux diffractometer in the temperature range from 1.8 to 52 K, with a wave-length λ=2.413 Å. The refinements of both crystal and magnetic structures were performed by the Rietveld program FULLPROF [8]. In the refinements the peak shape was simulated by a pseudo-Voigt function and the background was fitted with a fifth-degree polynomial function.

3. Results

The study of the crystallographic structure, refined from high resolution neutron diffraction data in the conventional *Pnma* space group, reveals an important distortion of the MnO_6 octahedra, due to the Jahn–Teller effect: the three Mn–O distances, Mn–O1, Mn–O2 and Mn–O2′ are, respectively, 1.9435(1), 1.9046(16) and 2.2224(17) Å. At temperatures above 90 K the susceptibility follows a Curie–Weiss behavior described by an effective paramagnetic moment μ_{eff}=10.7(1) μ_B per formula, being the interpolated paramagnetic temperature Θ_p=−17(1) K. The effective moment is lower than the expected figure for spin-only Mn^{3+} and Ho^{3+} (J=8), 11.5 μ_B. The negative paramagnetic temperature implies the presence of AFM exchange interactions. It is inferred from specific heat and magnetic measurements (Fig. 1) that $HoMnO_3$ presents an interesting magnetic phase diagram. First, it orders below T_N≈41 K, and another two magnetic transitions are observed at around T≈26 K and T≈6.5 K.

3.1. Magnetic structures

The evolution of the NPD patterns between 1.8 and 52 K is shown in Fig. 2. On decreasing temperature below 47.5 K, new reflections appear on positions forbidden for the Bragg reflections in the space group *Pnma*. These new peaks correspond to satellites defined by the propagation vector $\mathbf{k}=(k_x,0,0)$, indicating the transition to an incommensurate magnetic structure. As temperature diminishes, the position of the magnetic peaks varies, implying a change in the k_x component of the propagation vector. Its value progressively increases and reaches the commensurate value $k_x=1/2$ at T≈29 K. The commensurate propagation vector remains stable down to 1.8 K. Above 22 K, the magnetic ordering corresponds to the Mn^{3+} ions only. After checking all of the possible solutions given by the group theory, the best agreement with the experimental data is obtained for a modulated sine-wave structure, given by the magnetic mode $(C_x,0,0)$. The same mode is observed in the commensurate region. Fig. 3 shows the thermal evolution of the magnetic moments. Below 22 K, the Ho^{3+} magnetic moments also become ordered, adopting the magnetic structure $(A_x,0,C_z)$; at low temperatures (T<6.5 K) the Ho moments notably increase, as shown in Fig. 3, reaching the saturation value of 7.27(11) μ_B at 1.8 K. Fig. 4 schematically illustrates the magnetic structures in both incommensurate and commensurate regions, the last one including the AFM of the Ho^{3+} moments.

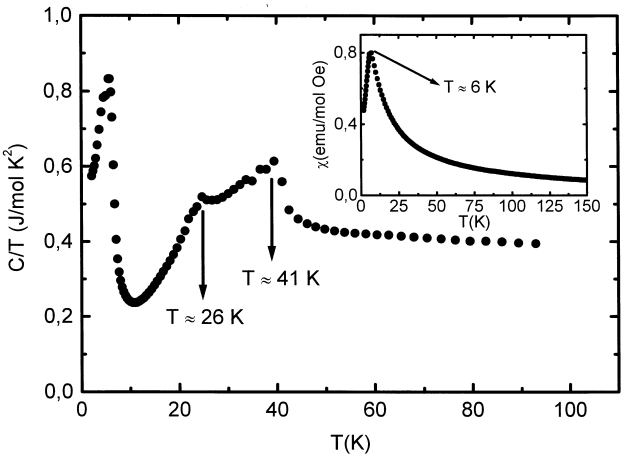

Fig. 1. Specific heat versus temperature curve. Inset: thermal variation of the susceptibility.

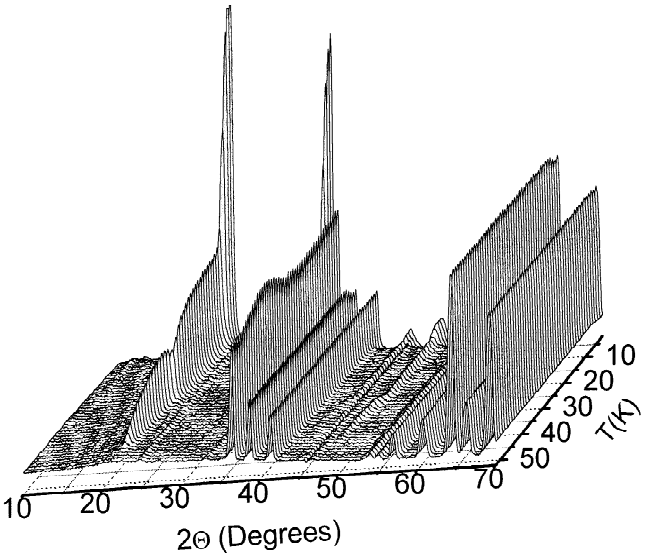

Fig. 2. Thermal evolution of the NPD patterns of $HoMnO_3$ collected in D20 (ILL).

4. Discussion

Neutron diffraction experimental results have emphasized that $HoMnO_3$ presents a very peculiar evolution of the magnetic structures in comparison with other orthorhombic manganites: for the larger rare-earth cations, $LaMnO_3$, $PrMnO_3$ and $NdMnO_3$, present a commensurate ground state ordered arrangement, whereas the smaller rare-earth perovskites, $TbMnO_3$ and $YMnO_3$, present an incommensurate magnetic structure down to 2 K [9,10];

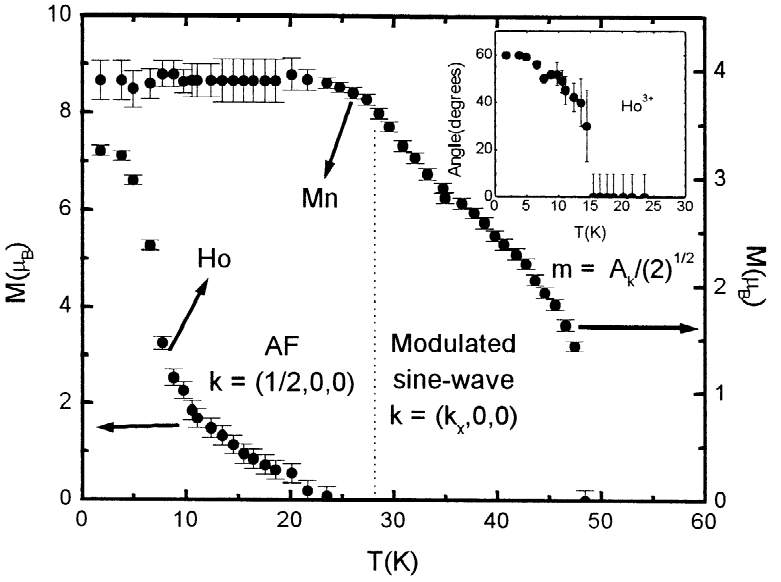

Fig. 3. Thermal variation of the ordered Mn^{3+} and Ho^{3+} magnetic moments. Inset: thermal evolution of the angle that the magnetic moment of the Ho^{3+} ions forms with the *a* axis.

$HoMnO_3$ is the first compound in which an incommensurate to commensurate transition has been observed.

It is noteworthy that the same kind of magnetic arrangement for Mn^{3+} moments, characterized by a $(C_x,0,0)$ mode, has already been reported for $TbMnO_3$ and $YMnO_3$ in the entire temperature range down to 1.8 K, exhibiting the same orientation along the *a* axis of the Mn magnetic moments. This AFM arrangement seems to be, thus, the stable ground state for small-sized rare-earth manganese perovskites. Let us point out that in all the series the magnetic anisotropy aligns the Mn magnetic moments along the *a* direction. The magnetic structure typified by $LaMnO_3$ has been interpreted as the result of the orbital ordering of e_g orbitals within each layer, giving rise to four FM interactions, according to the Goodenough-Kanamori [11] rules. The same kind of orbital ordering is presumably present in $HoMnO_3$, since the structural data (defined in the same space group) indicate a strong deformation of the MnO_6 octahedra, symptomatic of a cooperative Jahn–Teller distortion. However, the tilting of the MnO_6 octahedra increases from 24.8° for R=La to 34.7° for R=Tb, and finally to 36.5° for R=Ho. The validity of the Goodenough rules [11], dictating an FM interaction between occupied dz^2 orbitals rotated by 90°, requires a superexchange Mn–O–Mn angle close to 180°. For $HoMnO_3$, the ⟨Mn–O–Mn⟩ angle is 144.1°, which probably spoils the overlapping between Mn and O orbitals required to ensure the FM interaction with all the four neighboring Mn atoms. The weakening of the interactions to the nearest neighbors probably makes it possible that next-nearest neighbor interactions become important in the Hamiltonian determining the stable ground state. The presence of competing superexchange interactions of opposite sign can also be in the origin of the incommensurability observed in $HoMnO_3$ immediately below T_N. Finally, our results suggest that the ordering of Ho^{3+} moments is driven by superexchange Ho–O–Ho interactions: according to the mean-field approximation, the environment of Mn magnetic moments would give rise to a zero polarization at the Ho site, thus precluding a polarization effect from the exchange field of the moments of the Mn cations.

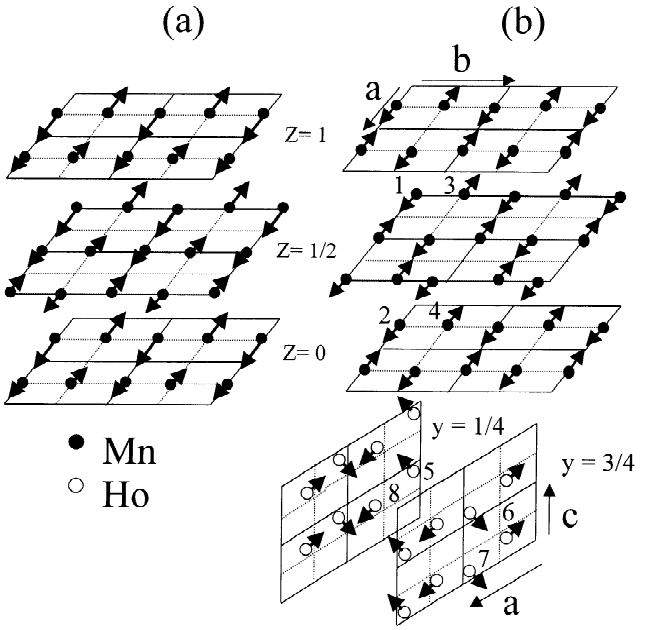

Fig. 4. Magnetic structures of $HoMnO_3$: (a) in the incommensurate region, 41 K>*T*>29 K, only Mn moments are ordered; (b) at *T*=1.8 K, in the commensurate region, also showing the AFM arrangement of Ho^{3+} moments.

5. Conclusions

By cooling from the paramagnetic state, T_N=41 K, an incommensurate sinusoidal modulated AFM ordering of the Mn^{3+} moments crystallizes, characterized by the wave-vector $\mathbf{k}=(k_x,0,0)$ (k_x=0.4 at 41 K) and defined by the magnetic mode (C_x,0,0). This structure is stable down to $T\approx$29 K, although the propagation vector continuously evolves in this region, finally adopting the commensurate value $\mathbf{k}=(1/2,0,0)$ at 29 K. Below $T\approx$22 K, Ho^{3+} magnetic moments also become ordered, adopting an AFM arrangement (A_x,0,C_z), superimposed to the ordered Mn sublattice. The magnetic ordering of Ho^{3+} ions is associated with Ho–O–Ho superexchange interactions. The different arrangement observed for the Mn moments with respect to the first members of the $RMnO_3$ series is probably related to the strong steric distortion of the structure, given by the small size of the R cation; the significant bending of the Mn–O–Mn angles prevents or reduces the strength of the expected FM couplings between nearest neighbors, enabling the interactions from next-nearest neighbors to play a non-negligible role in the stabilization of an intermediate incommensurate structure that finally evolves at lower temperatures to a commensurate (C_x,0,0) magnetic arrangement.

References

[1] R.M. Kusters, J. Singleton, D.A. Keen, R. McGreevy, W. Hayes, Physica B 155 (1989) 362.
[2] R. Von Helmolt, J. Wecker, B. Holzapfet, L. Schultz, K. Samwer, Phys. Rev. Lett. 71 (1993) 2331.
[3] T. Saitoh, A.E. Boucquet, T. Mizokawa, H. Namatame, A. Fujimori, M. Abbate, Y. Takeda, M. Takano, Phys. Rev. B 51 (1995) 13942.
[4] F. Moussa, M. Hennion, J. Rodríguez-Carvajal, H. Moudden, Phys. Rev. B 54 (1996) 15149.
[5] S. Quezel, J. Rossat-Mignod, E.F. Bertaut, Solid State Commun. 14 (1974) 941.
[6] H.W. Brinks, H. Fejllvag, A. Kjekshus, J. Solid State Chem. 129 (1997) 334.
[7] J.A. Alonso, M.J. Martínez-Lope, M.T. Casais, M.T. Fernández-Díaz, Inorg. Chem. 39 (2000) 917.
[8] J. Rodríguez-Carvajal, Physica B 192 (1993) 55.
[9] S. Quezel, F. Tcheou, J. Rossat-Mignot, G. Quezel, E. Roudaut, Physica B 86–88 (1977) 916.
[10] S. Quezel, J. Rossat-Mignot, E.F. Bertaut, Solid State Commun. 14 (1974) 94.
[11] J.B. Goodenough, Phys. Rev. 100 (1955) 564.